

Supplemental Information for
Molecular Characterization of Brown Carbon in Biomass Burning
Aerosol Particles

Peng Lin,¹ Paige K. Aiona,² Ying Li,^{3,5} Manabu Shiraiwa,^{2,3} Julia Laskin,⁴ Sergey A. Nizkorodov,²
Alexander Laskin^{1*}

¹ *Environmental Molecular Sciences Laboratory, Pacific Northwest National Laboratory, Richland, WA, 99354, United States*

² *Department of Chemistry, University of California, Irvine, CA, 92697, United States*

³ *Multiphase Chemistry Department, Max Planck Institute for Chemistry, Mainz, 55128, Germany*

⁴ *Physical Sciences Division, Pacific Northwest National Laboratory, Richland, WA, 99354, United States*

⁵ *National Institute for Environmental Studies, Tsukuba-City, Ibaraki, 305-8506 Japan*

*email: alexander.laskin@pnnl.gov

Phone: +1 509 371-6129

Appendix I: Details of the experimental section.

Table S1. A list of elemental formulas of BrC chromophores found in the four BBOA samples.

Figure S1. The total ion chromatograms (TIC) acquired in the (+)ESI mode and (–)ESI mode for BBOA samples from burning of ponderosa pine (PP).

Figure S2. The total ion chromatograms (TIC) acquired in the (+)ESI mode and (–)ESI mode for BBOA samples from burning of black spruce (BS).

Figure S3. The total ion chromatograms (TIC) acquired in the (+)ESI mode and (–)ESI mode for BBOA samples from burning of peat (PT).

Figure S4. The total ion chromatograms (TIC) acquired in the (+)ESI mode and (–)ESI mode for BBOA samples from burning of sawgrass (SG).

Figure S5. Examples of PDA and MS results obtained for chromophores eluting at RT = 15.0 min and RT = 50.6 min, respectively.

Figure S6. An example demonstrating the method used for identification of organic compounds responsible for light absorption of major chromophore #20 (RT = 50.6 min) in Figure 3 of the main text.

Figure S7. UV-Vis spectra of the strong chromophores observed in SG BBOA.

Figure S8. Tentative molecular structures of chromophores identified in SG BBOA.

Figure S9. 3D-plot of HPLC/PDA chromatogram of BBOA from peat (PT) burning.

Figure S10. 3D-plot of HPLC/PDA chromatogram of BBOA from ponderosa pine (PP) burning.

Figure S11. 3D-plot of HPLC/PDA chromatogram of BBOA from black spruce (BS) burning.

Figure S12. Tentative molecular structures of chromophores identified in PT, PP, or BS BBOA.

Figure S13. 10-40 min segments of HPLC/PDA chromatograms shown as density maps indicating strong BrC chromophores in the PT, PP, and BS BBOA samples.

Appendix II: Method for Testing the Stability of BrC Chromophores in Solution

Figure S14. Spectra of actinometer at each photolysis time and change in absorbance at 458 nm as a function of time which was used to calculate the lamp flux.

Figure S15. Left: Absorption spectra of the PT BBOA sample before and after UV irradiation, and the effect of the irradiation on the AAE of the PT BBOA.

Table S2. Half-lives ($t_{1/2}$) for the disappearance of the 300 nm absorbance measured in the experimental setup and estimated under the 24-hour averaged irradiation conditions in Los Angeles on June 30.

Figure S16. Change in absorbance at 300 nm as a function of time exposed to the lamp for PP and PT BBOA samples.

Figure S17. Solar spectral flux density in Los Angeles, CA on June 30 at 20 hours GMT (maximum flux).

Appendix I: Details of the Experimental Section

BBOA samples were collected during the fourth Fire Lab at Missoula Experiment (FLAME-4) conducted at the U.S. Forest Service Fire Science Laboratory in Missoula, MT, where a series of laboratory measurements and aerosol sampling of biomass burning emissions were performed in October and November of 2012.¹ This paper focuses on the BrC content in BBOA samples from four different biofuels: sawgrass (SG), peat (PT), ponderosa pine (PP), and black spruce (BS). They are representative biomass materials consumed by fires in grassland, peatland, and forest areas.^{2,3} The FLAME-4 was designed to investigate fire emissions under the conditions representative of “real-world” biomass burning activities.¹ A fire-integrated modified combustion efficiency (MCE) was calculated to characterize the relative amount of smoldering and flaming combustion phase that occurred over the course of each fire.¹ MCE of 1 corresponds to an ideal flaming combustion that converts all carbon in the fuel to CO₂; MCE below 1 corresponds to an incomplete, smoldering combustion that results in BBOA. The averaged MCE values were reported as 0.96±0.004, 0.81±0.09, 0.91±0.03, and 0.96±0.008, for the burning of SG, PT, PP and BS, respectively.² These differences in MCE may result from many factors such as structure of the fuel assembly prior to its ignition, moisture content, and environmental variables.^{4,5} Thus, although the intent of this paper is to characterize BrC emitted from different biofuels, it should be noted that the chemical composition of BrC may also depend on the variables that were not controlled in this study.

Smoke particles were collected onto aluminum foil substrates using a 10-stage Micro-Orifice Uniform Deposit Impactor (MOUDI, MSP, Inc). Samples on the 6th and 7th impactor stages were combined together for the analysis. The particle size range in these samples was 0.32-1.0 μm (aerodynamic diameter). Solvent extracts were prepared by ultrasonic extraction of the BBOA samples from aluminum foils in 2 mL of LC/MS grade acetonitrile. The extracts were filtered using syringe filters with 0.45 μm PTFE membrane to remove insoluble fractions. The resulting solutions were first concentrated through evaporation under N₂ flow to a volume of ~ 50 μL, and then ~200 μL of ultrapure water was added to make the solvent composition compatible with the initial setting of solvent gradient used for HPLC analysis. The change in filter color from brown to colorless suggests that the majority of light-absorbing compounds were extracted in the solution.

Solutions of BBOA samples were analyzed using an HPLC/PDA/HRMS platform.^{6,7} The platform consists of a Surveyor Plus system (including a quaternary LC pump, an auto sampler and a PDA detector), a standard IonMAXTM electrospray ionization (ESI) source, and a high resolution LTQ-Orbitrap mass spectrometer (all modules are from Thermo Electron, Inc). The separation was performed on a reverse-phase column (Luna C18, 2 × 150 mm, 5 μm particles, 100 Å pores, Phenomenex, Inc.). The binary solvent “A” included water with 0.05% v/v formic

acid and solvent “B” included LC/MS grade acetonitrile with 0.05% v/v formic acid. Gradient elution was performed by the A/B mixture at a flow rate of 200 $\mu\text{L}/\text{min}$: 0–3 min hold at 10% of B, 3–53 min linear gradient to 90% B, 53–80 min hold 90% B, 80–81 min return back to 10% B held for 100 min to recondition the column and make it ready for injection of the next sample. UV-Vis absorption was measured using the PDA detector over the wavelength range of 200 to 700 nm. The spectrum of the unseparated mixture was also measured with the column removed at the same flow rate of the A/B solvent with 10% B. The ESI settings were as follows: 4.0 kV spray potential, 35 units of sheath gas flow, 10 units of auxiliary gas flow, and 8 units of sweep gas flow. ESI/HRMS data was acquired in both positive and negative modes.

Xcalibur (Thermo Scientific) was used to acquire raw data. The HPLC/PDA/HRMS data were processed with an open source software toolbox, MZmine 2 (<http://mzmine.github.io/>), to perform peak deconvolution and chromatogram construction.⁸ Analysis and assignments of MS peaks were performed using a suite of Microsoft Excel macros developed in our group that enable background subtraction, first and second-order mass defect analysis and grouping of homologous peaks.⁹ Elemental formulas of one representative peak from each group were assigned using MIDAS molecular formula calculator (<http://magnet.fsu.edu/~midas/>). Formula assignments were performed using the following constraints: $C \leq 100$, $H \leq 200$, $N \leq 3$, $O \leq 50$, $S \leq 1$ and $Na \leq 1$. The aromatic index (AI)^{10, 11} values were calculated using the equation $AI = [1 + c - o - s - 0.5h] / (c - o - n - s)$, where c , h , o , n and s correspond to the number of carbon, hydrogen, oxygen, nitrogen and sulfur atoms in the neutral formula, respectively. The double-bond equivalent (DBE) values of the neutral formulas were calculated using the equation: $DBE = c - h/2 + n/2 + 1$. The data used for “molecular corridors” analysis^{12, 13} were obtained through direct infusion ESI-HRMS analysis of the samples and processed using the same protocols.⁹

Table S1. A list of elemental formulas of BrC chromophores found in the four BBOA samples: sawgrass (SG), peat (PT), ponderosa pine (PP), and black spruce (BS). RT = retention time, DBE = double bond equivalent. Some peaks were detected in the (+)ESI mode, some in the (-)ESI mode, and some in both. The peak numbers are shown in chromatograms in Figures S7-S9. Multiple assignments are possible for the same chromatographic peak, as shown in the table

BBOA	Peak #	RT (min)	Formula	DBE	ESI mode (+/-)
<i>BBOA sample collected from burning of sawgrass (SG)</i>					
SG	1	15.1	C ₆ H ₅ O ₄ N	5	-
SG	2	18.1	C ₈ H ₇ O ₄ N	6	-
SG	3	19.3	C ₁₃ H ₈ O ₂	10	+
SG	4	20.4	C ₇ H ₇ O ₄ N	5	-
SG	5	21.7	C ₈ H ₇ O ₃ N	6	-
SG	6	24.6	C ₉ H ₇ O ₄ N	7	-
			C ₁₃ H ₈ O	10	+
SG	7	26.9	C ₁₀ H ₇ O ₃ N	8	-
SG	8	28.9	C ₁₁ H ₉ O ₃ N	8	-
SG	9	31.8	C ₁₂ H ₁₁ O ₃ N	13	-
			C ₁₉ H ₁₀ O ₂	15	+
SG	10	33.1	C ₁₆ H ₉ O ₃ N	13	-
			C ₁₃ H ₁₃ O ₃ N	8	-
SG	11	33.8	C ₁₉ H ₁₀ O	15	+
			C ₁₈ H ₈ O ₃	15	+
SG	12	34.7	C ₂₀ H ₁₀ O ₂	16	+
			C ₁₉ H ₁₀ O	15	+
SG	13	35.4	C ₂₁ H ₁₁ N	17	+
			C ₁₇ H ₁₀ O	13	+
SG	14	38.2	C ₂₁ H ₁₂ O	16	+
SG	15	39.3	C ₃₁ H ₃₀ O ₅	17	-
SG	16	43.3	C ₂₆ H ₁₂ O ₂	21	+
			C ₂₂ H ₁₂ O ₂	17	+
			C ₂₃ H ₁₃ N	18	+
SG	17	46.0	C ₂₁ H ₁₃ N	16	+
			C ₂₃ H ₁₂ O	18	+
SG	18	46.8	C ₁₈ H ₂₇ O ₅ N	9	-
			C ₂₃ H ₃₁ O ₄ N	9	-
			C ₃₁ H ₃₀ O ₄	17	+
			C ₃₄ H ₂₆ O ₃	22	+
SG	19	49.2	C ₂₅ H ₃₄ O ₂	9	+
			C ₂₆ H ₃₆ O ₉	9	-
SG	20	50.6	C ₂₅ H ₃₆ O ₂	8	-
			C ₂₇ H ₃₉ O ₂ N	9	+
			C ₂₂ H ₃₄ O ₆ N ₂	7	+
			C ₄₈ H ₆₆ O ₄ N ₄	18	+

BBOA sample collected from burning of peat (PT)					
PT	1	10.2	C ₈ H ₈ O ₃	5	-
			C ₉ H ₈ O ₃	6	-
PT	2	10.9	C ₉ H ₁₀ O ₄	5	-/+
PT	3	13.7	C ₁₀ H ₁₂ O ₄	5	-/+
PT	4	14.6	C ₉ H ₇ O ₃ N	7	-
PT	5	18.6	C ₁₀ H ₈ O ₄	7	-
			C ₉ H ₆ O ₃	7	-
PT	6	18.9	C ₁₃ H ₁₀ O ₆	9	-/+
PT	7	21.8	C ₁₃ H ₁₂ O ₄	8	-
PT	8	22.2	C ₁₁ H ₁₀ O ₄	7	-/+
PT	9	22.8	C ₁₃ H ₈ O ₅	10	-/+
			C ₁₄ H ₈ O ₇	11	-/+
			C ₁₇ H ₁₄ O ₇	11	-/+
PT	10	23.8	C ₁₄ H ₁₀ O ₅	10	-/+
			C ₁₄ H ₁₀ O ₆	10	-/+
PT	11	24.5	C ₁₂ H ₁₀ O ₂	8	-/+
			C ₁₄ H ₁₄ O ₄	8	-/+
PT	12	25.4	C ₁₃ H ₈ O ₆	10	-/+
PT	13	26.2	C ₁₇ H ₁₂ O ₆	12	-/+
PT	14	31.0	C ₁₈ H ₁₆ O ₆	11	-/+
			C ₁₉ H ₁₈ O ₆	11	-/+
PT	15	35.3	C ₁₈ H ₁₆ O ₅	11	-/+
PT	16	39.3	C ₁₉ H ₁₈ O ₅	11	-/+
PT	17	41.9	C ₂₀ H ₂₀ O ₅	11	-/+
			C ₂₂ H ₂₀ O ₆	13	-/+
PT	18	43.1	C ₂₃ H ₂₂ O ₆	13	-/+
			C ₂₃ H ₂₄ O ₆	12	-/+
PT	19	44.0	C ₂₇ H ₂₆ O ₅	15	-/+
PT	20	46.2	C ₂₄ H ₂₂ O ₅	14	-/+
			C ₂₈ H ₂₈ O ₆	15	-/+
BBOA sample collected from burning of ponderosa pine (PP)					
PP	1	10.0	C ₈ H ₈ O ₃	5	-
PP	2	11.4	C ₇ H ₆ O ₃	5	-
PP	3	12.8	C ₁₀ H ₁₀ O ₃	6	-
			C ₁₀ H ₈ O ₄	7	-
PP	4	13.7	C ₉ H ₈ O ₃	6	-
			C ₈ H ₈ O ₄	5	-
PP	5	14.5	C ₉ H ₆ O ₃	7	-
			C ₉ H ₇ O ₃ N	7	-
PP	6	15.9	C ₇ H ₇ O ₅ N	5	-
PP	7	16.3	C ₁₂ H ₁₂ O ₄	7	+
PP	8	16.8	C ₂₀ H ₂₂ O ₄	10	+
			C ₂₀ H ₂₄ O ₅	9	+
PP	9	19.3	C ₈ H ₉ O ₅ N	5	-
PP	10	19.7	C ₁₅ H ₁₄ O ₄	9	-

PP	11	22.8	C ₁₅ H ₁₀ O ₆	11	-
			C ₁₉ H ₂₀ O ₅	10	-/+
PP	12	23.1	C ₁₆ H ₁₂ O ₇	11	-
PP	13	23.7	C ₁₇ H ₁₄ O ₇	11	-/+
PP	14	24.4	C ₁₄ H ₁₄ O ₄	8	-
			C ₁₅ H ₁₂ O ₄	10	-
PP	15	26.0	C ₁₇ H ₁₄ O ₅	11	-
PP	16	26.2	C ₁₆ H ₁₂ O ₆	11	-
PP	17	27.2	C ₁₇ H ₁₄ O ₆	11	-/+
PP	18	27.8	C ₁₅ H ₁₆ O ₄	8	-/+
PP	19	32.0	C ₁₈ H ₁₆ O ₄	11	-
PP	20	35.3	C ₂₀ H ₂₆ O ₃	8	+
BBOA sample collected from burning of black spruce (BS)					
BS	1	10.0	C ₈ H ₈ O ₃	5	-/+
BS	2	10.4	C ₆ H ₅ O ₅ N	5	-
BS	3	12.7	C ₁₁ H ₁₂ O ₄	6	-
			C ₁₀ H ₈ O ₄	7	-
BS	4	13.3	C ₈ H ₈ O ₂	5	-
BS	5	13.7	C ₉ H ₈ O ₃	6	-
			C ₁₅ H ₁₆ O ₇	8	-
BS	6	14.5	C ₉ H ₆ O ₃	7	-
			C ₉ H ₇ O ₃ N	7	-
BS	7	15.0	C ₆ H ₅ O ₄ N	5	-
BS	8	15.6	C ₁₀ H ₁₀ O ₄	6	-
BS	9	15.8	C ₇ H ₇ O ₅ N	5	-
BS	10	16.8	C ₂₀ H ₂₂ O ₄	10	+
			C ₂₀ H ₂₄ O ₅	9	+
BS	11	18.0	C ₇ H ₇ O ₄ N	5	-
			C ₈ H ₇ O ₄ N	6	-
BS	12	19.7	C ₁₅ H ₁₄ O ₄	9	-
BS	13	22.5	C ₁₇ H ₁₄ O ₈	11	-
BS	14	22.8	C ₁₅ H ₁₀ O ₆	11	-/+
			C ₁₉ H ₂₀ O ₅	10	-
BS	15	23.1	C ₁₆ H ₁₂ O ₇	11	-
BS	16	23.7	C ₁₇ H ₁₄ O ₇	11	-
BS	17	23.9	C ₁₄ H ₁₂ O ₃	9	-
BS	18	24.4	C ₁₄ H ₁₄ O ₄	8	-
BS	19	26.2	C ₁₆ H ₁₄ O ₄	10	-
BS	20	26.7	C ₁₇ H ₁₄ O ₆	8	-

PP BBOA

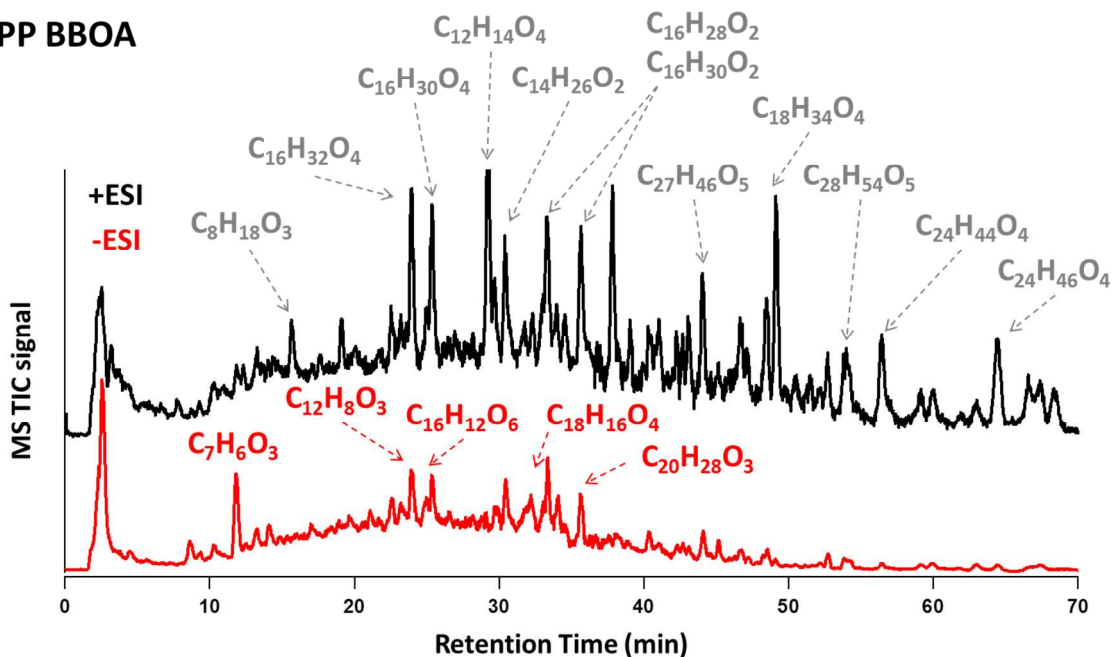


Figure S1. The total ion chromatograms (TIC) acquired in the (+)ESI mode (black) and (-)ESI mode (red) for BBOA samples from burning of ponderosa pine (PP). The (+)ESI signal is offset linearly from the (-)ESI signal for better display. Molecular formulas in red color denote aromatic compounds observed solely in the (-)ESI mode and representing potential BrC chromophores. Molecular formulas in gray color denote aliphatic compounds observed solely in the (+)ESI mode; they are unlikely to be BrC chromophores.

BS BBOA

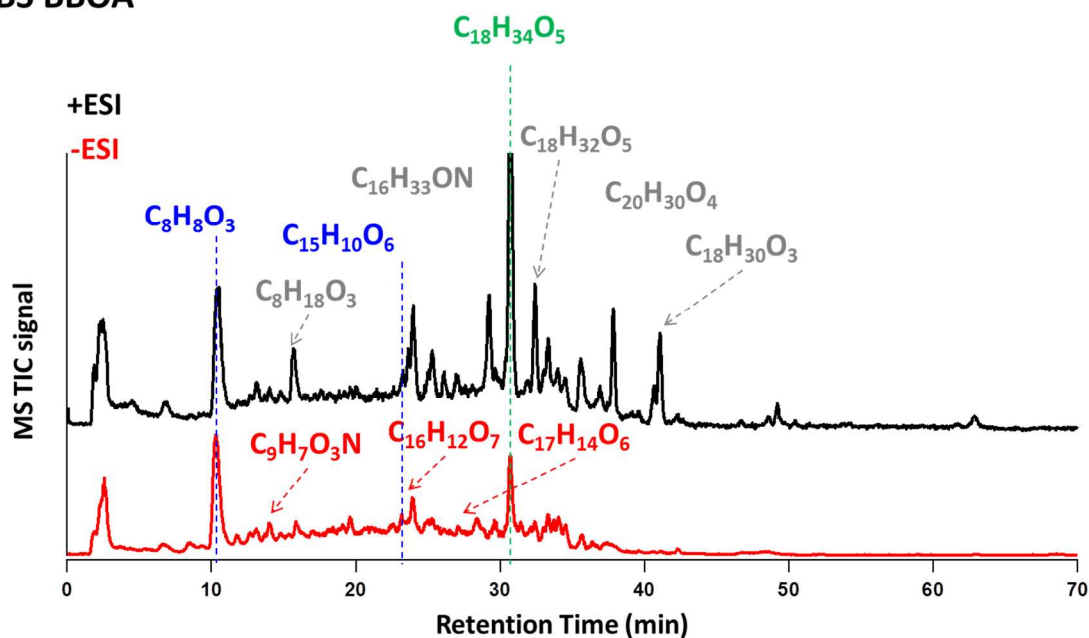


Figure S2. The total ion chromatograms (TIC) acquired in the (+)ESI mode (black) and (-)ESI mode (red) for BBOA samples from burning of black spruce (BS). The (+)ESI signal is offset linearly from the (-)ESI signal for better display. Molecular formulas in red color denote aromatic compounds observed solely in the (-)ESI mode and representing potential BrC chromophores. Molecular formulas in gray color denote aliphatic compounds observed solely in the (+)ESI mode; they are unlikely to be BrC chromophores. Molecular formulas in blue color denote aromatic compounds observed in both modes and are potential BrC chromophores. Molecular formulas in green color denote aliphatic compounds observed in both modes and are unlikely BrC chromophores.

PT BBOA

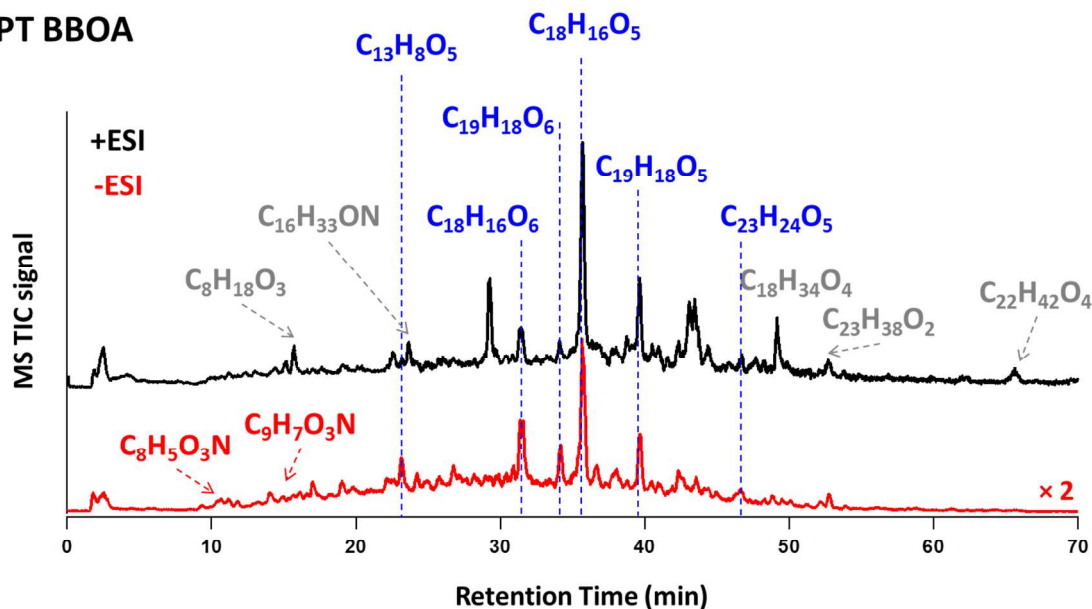


Figure S3. The total ion chromatograms (TIC) acquired in the (+)ESI mode (black) and (–)ESI mode (red) for BBOA samples from burning of peat (PT). The signal of the (–)ESI mode is multiplied by a factor of 2 and the (+)ESI signal is offset linearly from the (–)ESI signal for better display. Molecular formulas in red color denote aromatic compounds observed solely in the (–)ESI mode and representing potential BrC chromophores. Molecular formulas in gray color denote aliphatic compounds observed solely in the (+)ESI mode and are unlikely BrC chromophores. Molecular formulas in blue color denote aromatic compounds observed in both modes and are potential BrC chromophores.

SG BBOA

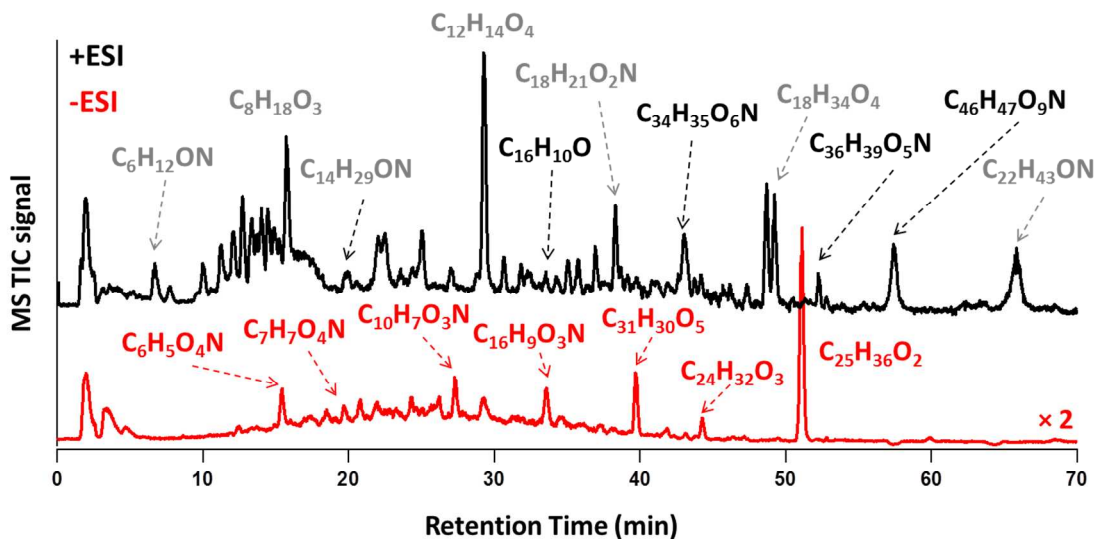


Figure S4. The total ion chromatograms (TIC) acquired in the (+)ESI mode (black) and (-)ESI mode (red) for BBOA samples from burning of sawgrass (SG). The signal in the (-)ESI mode is multiplied by a factor of 2 and the (+)ESI signal is offset linearly from the (-)ESI signal for better display. Molecular formulas in red color denote aromatic compounds observed solely in the (-)ESI mode and representing potential BrC chromophores. Molecular formulas in gray color denote aliphatic compounds observed solely in the (+)ESI mode and are unlikely BrC chromophores. Molecular formulas in black color denote aromatic compounds observed solely in positive ESI mode and are potential BrC chromophores.

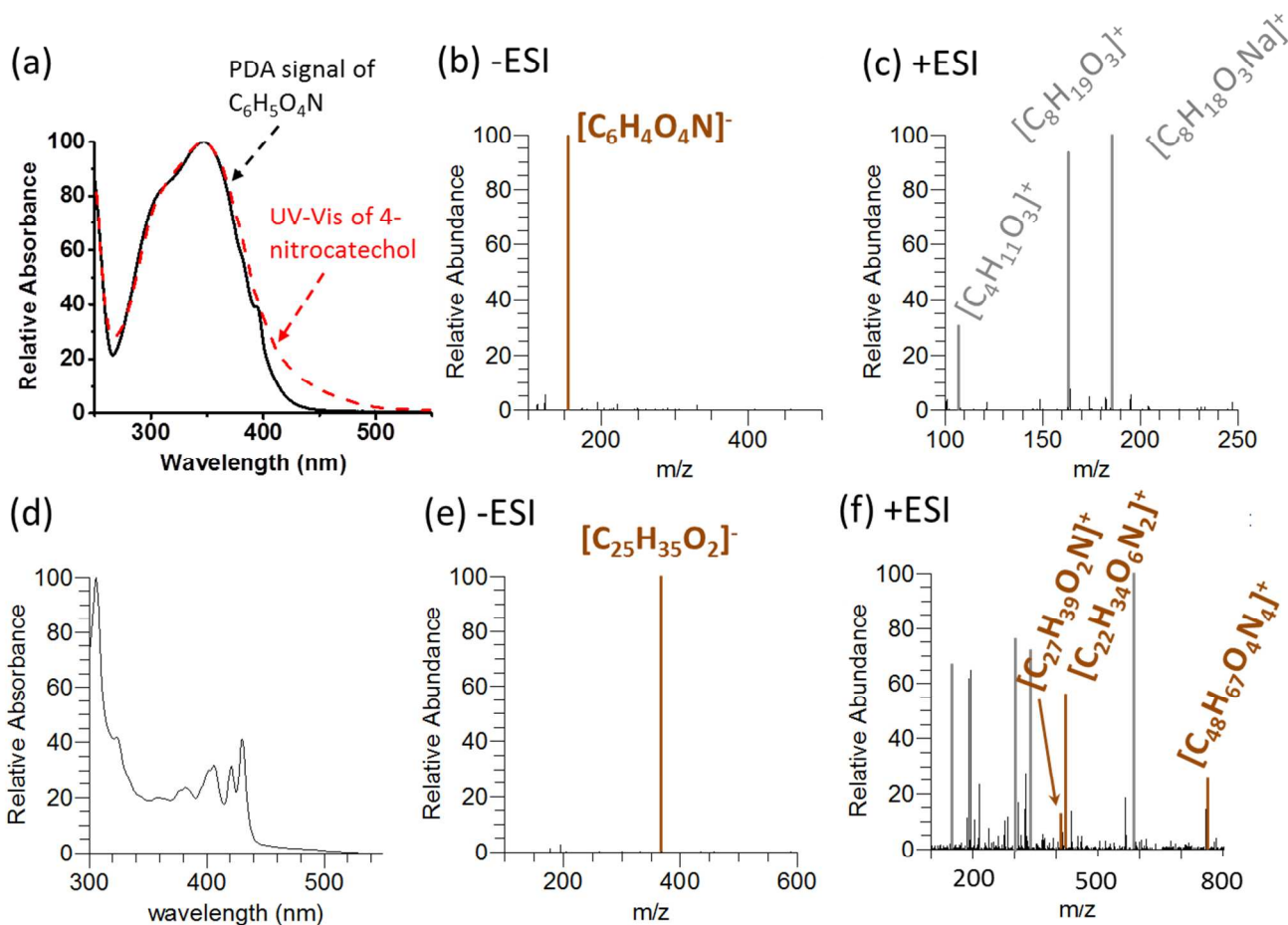


Figure S5. Examples of PDA and MS results obtained for chromophores (a-c) #2 and (d-f) #19 eluting at RT = 15.0 min and RT = 50.6 min, respectively. UV-Vis spectra of chromophores (a) #2 and (d) #19 eluting and their corresponding mass spectra acquired in the (-)ESI mode (b, e) and (+)ESI mode (c, f). Ions shown in brown color denote potential BrC chromophores with high double bond equivalent (DBE) values. Ions shown in gray color denote compounds with low DBE values that are unlikely to be BrC chromophores. The UV-Vis spectrum of 4-nitrocatechol (red dash line) was digitalized from reference 52.

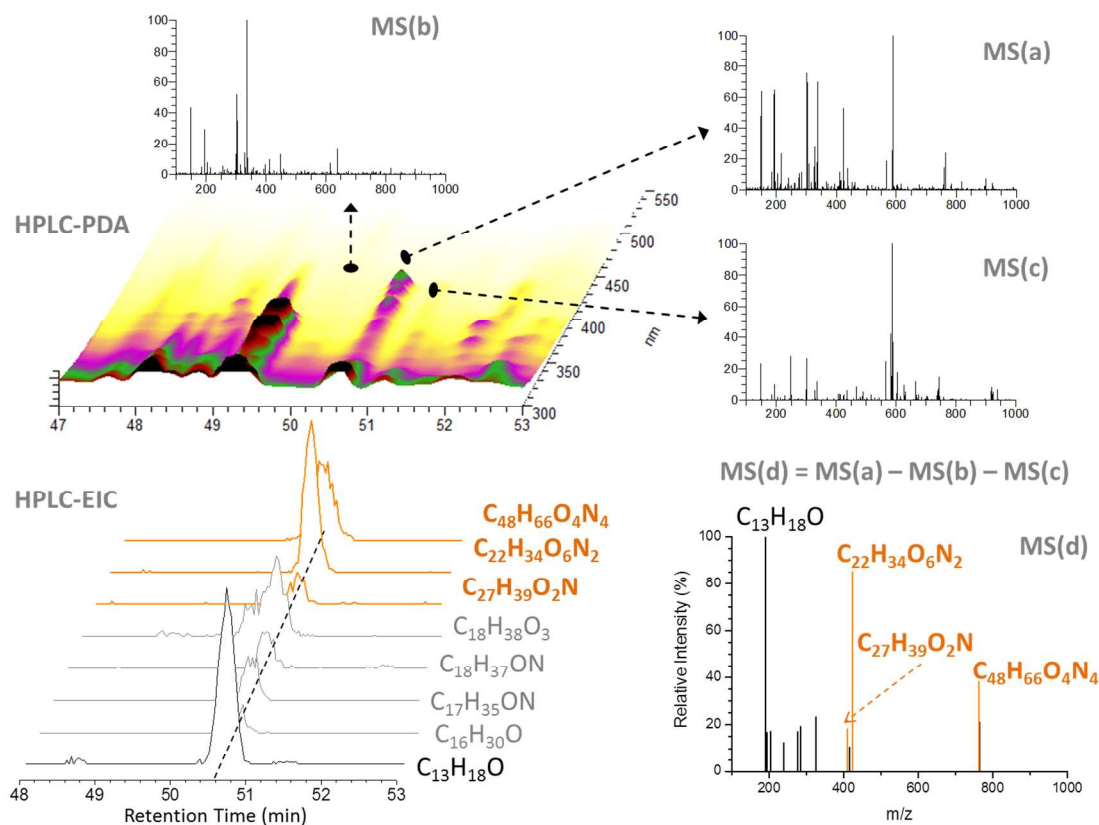


Figure S6. An example demonstrating the method used for identification of organic compounds responsible for light absorption of major chromophore #20 (RT = 50.6 min) in Figure 3 of the main text. MS(a) shows the mass spectrum corresponding to the absorption peak position as denoted on the color coded HPLC-PDA chromatogram. MS(b) and MS(c) show the mass spectra acquired before and after the corresponding PDA absorption peak. MS(d) shows the difference mass spectrum obtained by removing peaks present in MS(b) and MS(c) from MS(a). The bottom left panel displays the extracted ion chromatograms (EICs) of the compounds co-eluting at 50.6 min.

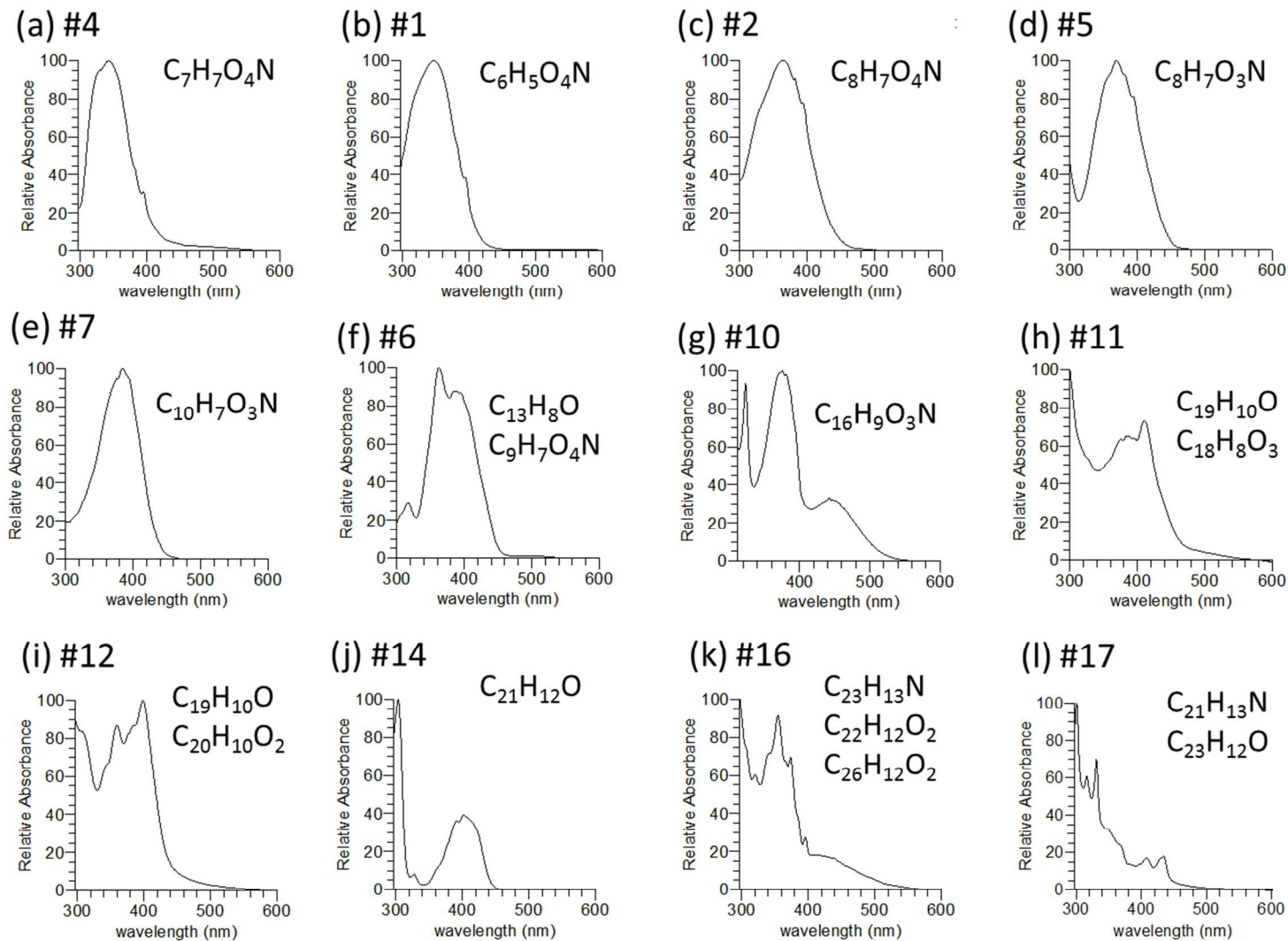


Figure S7. UV-Vis spectra of the strong chromophores (peak # of PDA record) observed in SG BBOA.

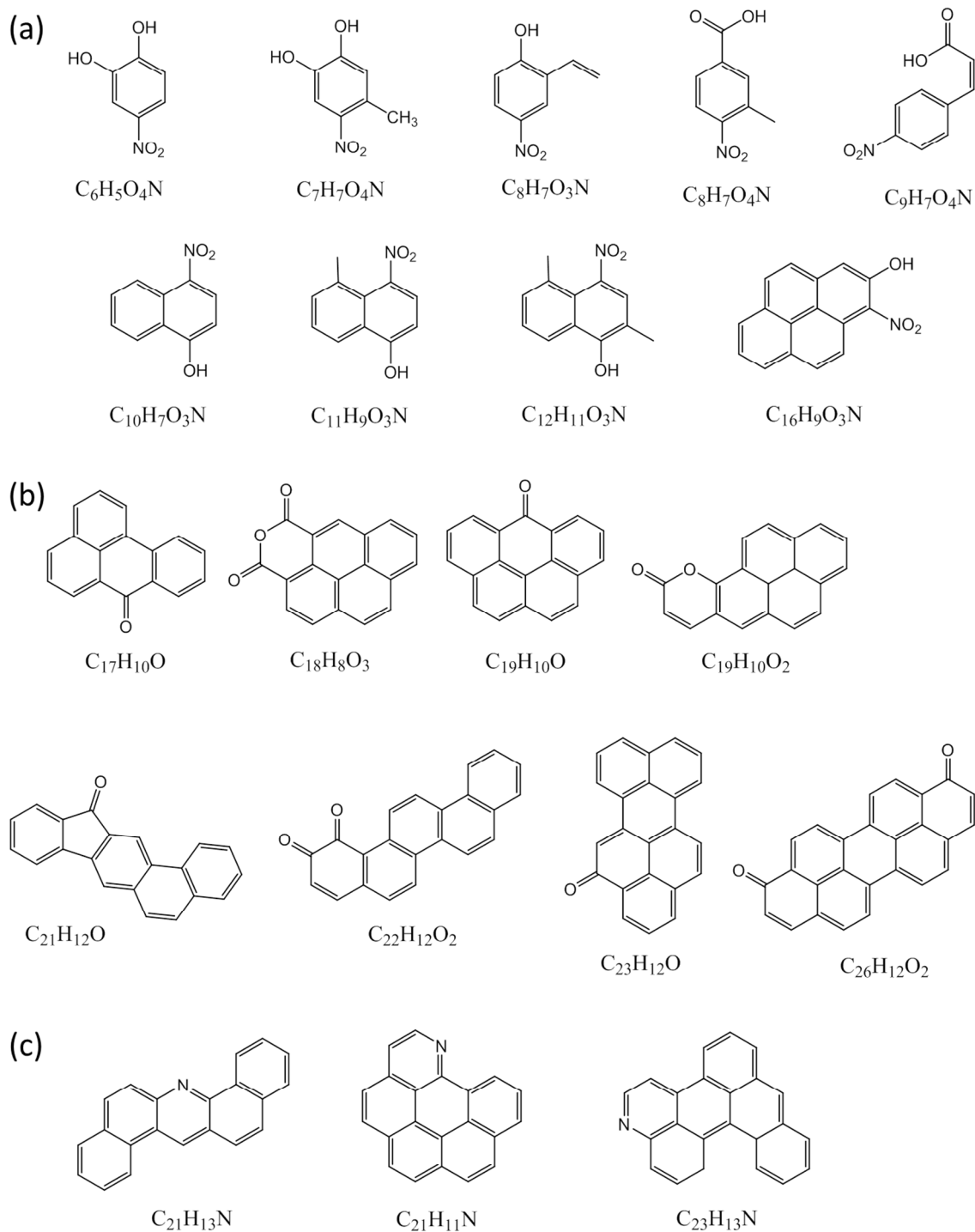


Figure S8. Tentative molecular structures of chromophores identified in SG BBOA: (a) nitro- and hydroxyl- substituted phenols and PAHs, (b) oxygenated and O-heterocyclic PAHs, (c) N-heterocyclic PAHs.

PT BBOA

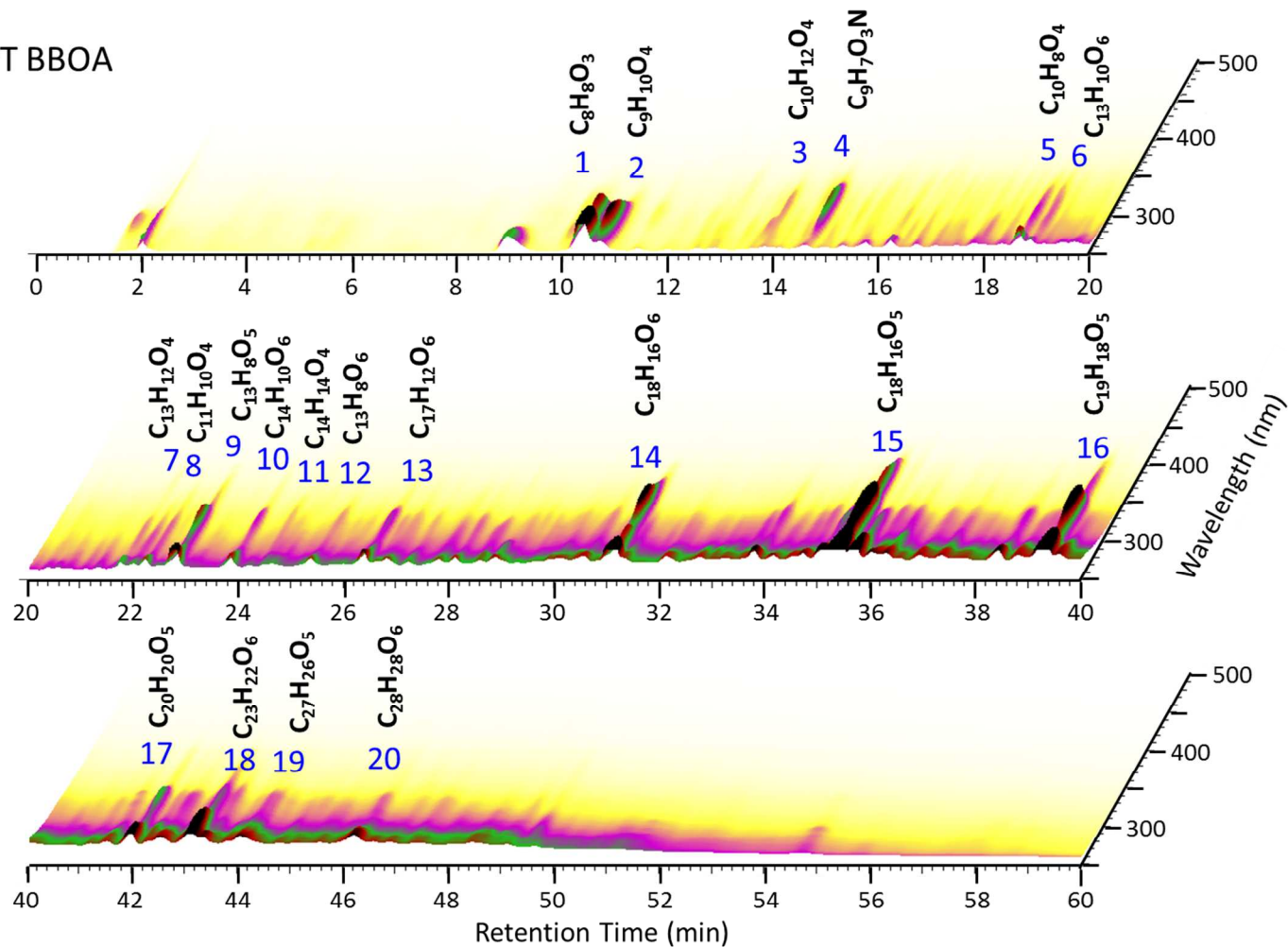


Figure S9. 3D-plot of HPLC/PDA chromatogram of BBOA from peat (PT) burning. The peaks are labelled by the peak numbers and by the formulas of the most probable chromophores from Table S1.

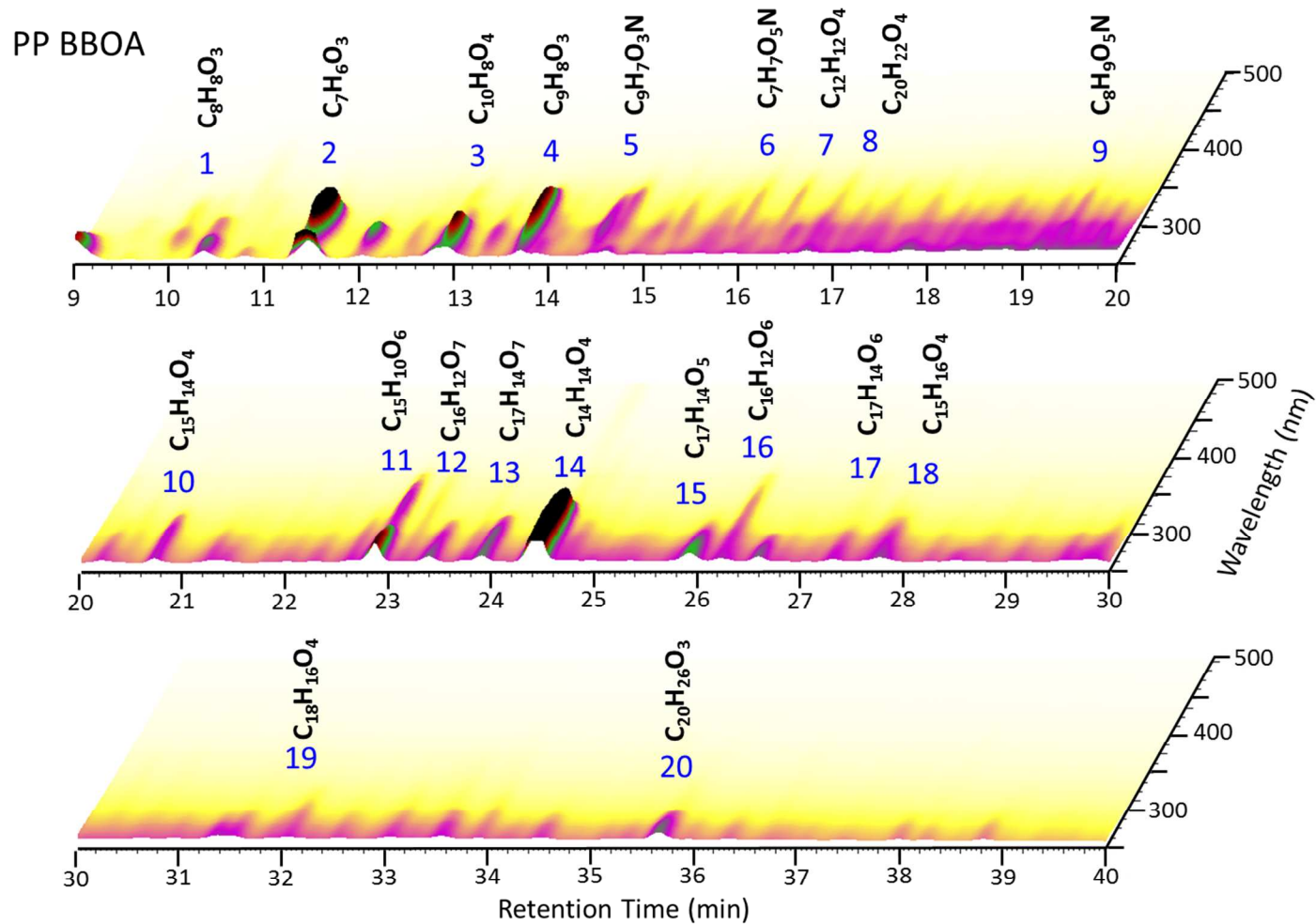


Figure S10. 3D-plot of HPLC/PDA chromatogram of BBOA from ponderosa pine (PP) burning. The peaks are labelled by the peak numbers and by the formulas of the most probable chromophores from Table S1.

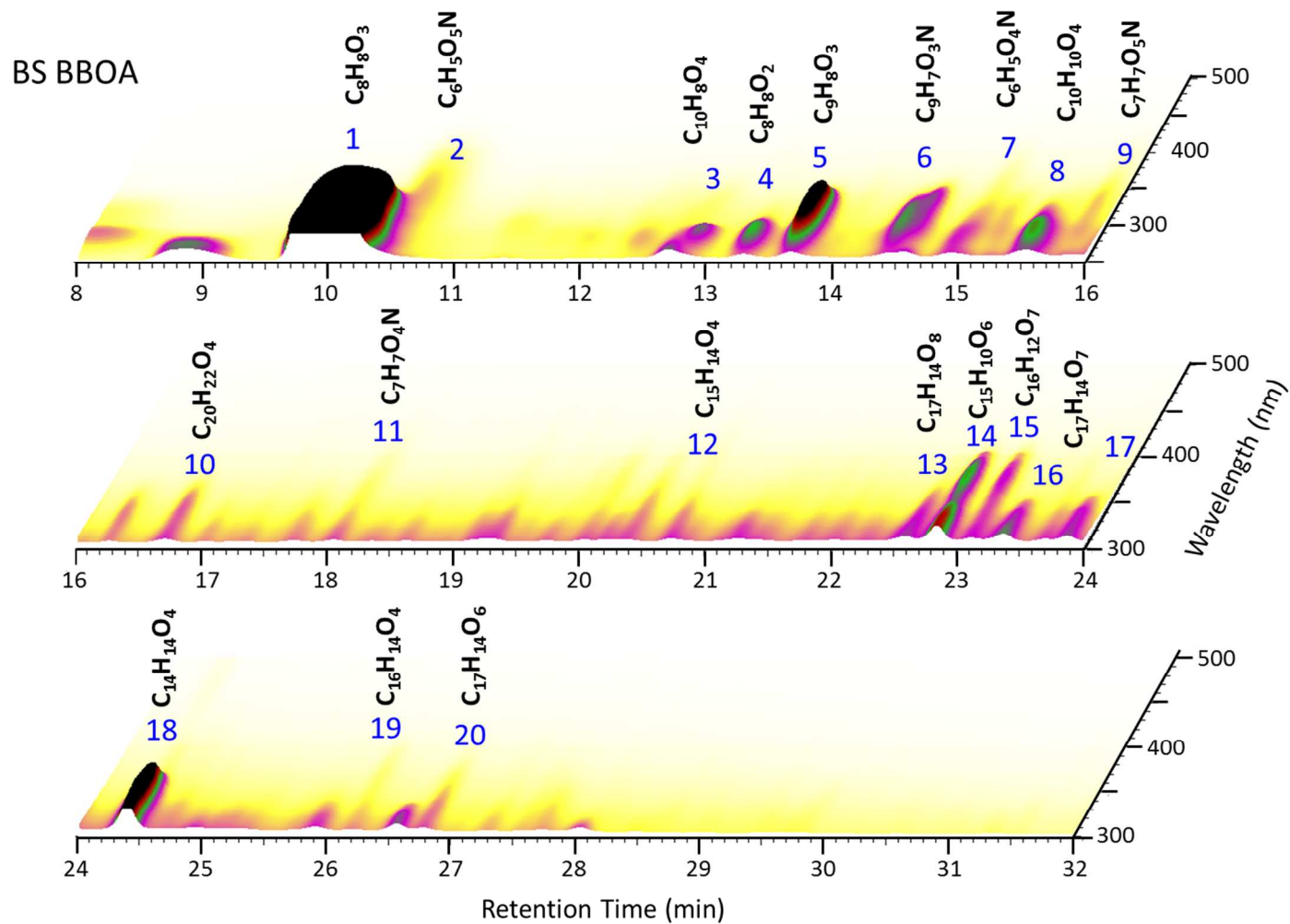


Figure S11. 3D-plot of HPLC/PDA chromatogram of BBOA from black spruce (BS) burning. The peaks are labelled by the peak numbers and by the formulas of the most probable chromophores from Table S1.

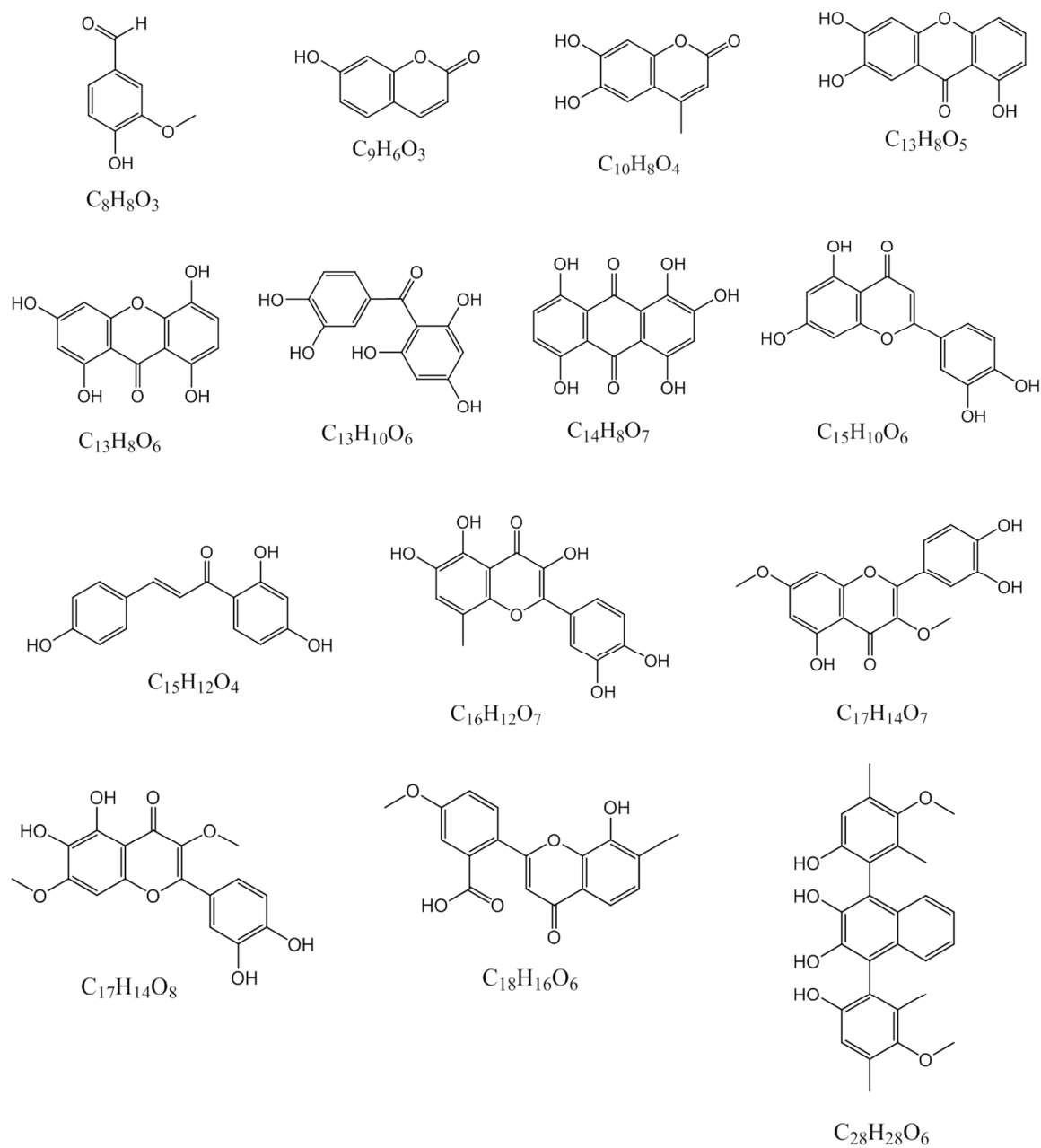


Figure S12. Tentative molecular structures of chromophores identified in PT, PP, or BS BBOA.

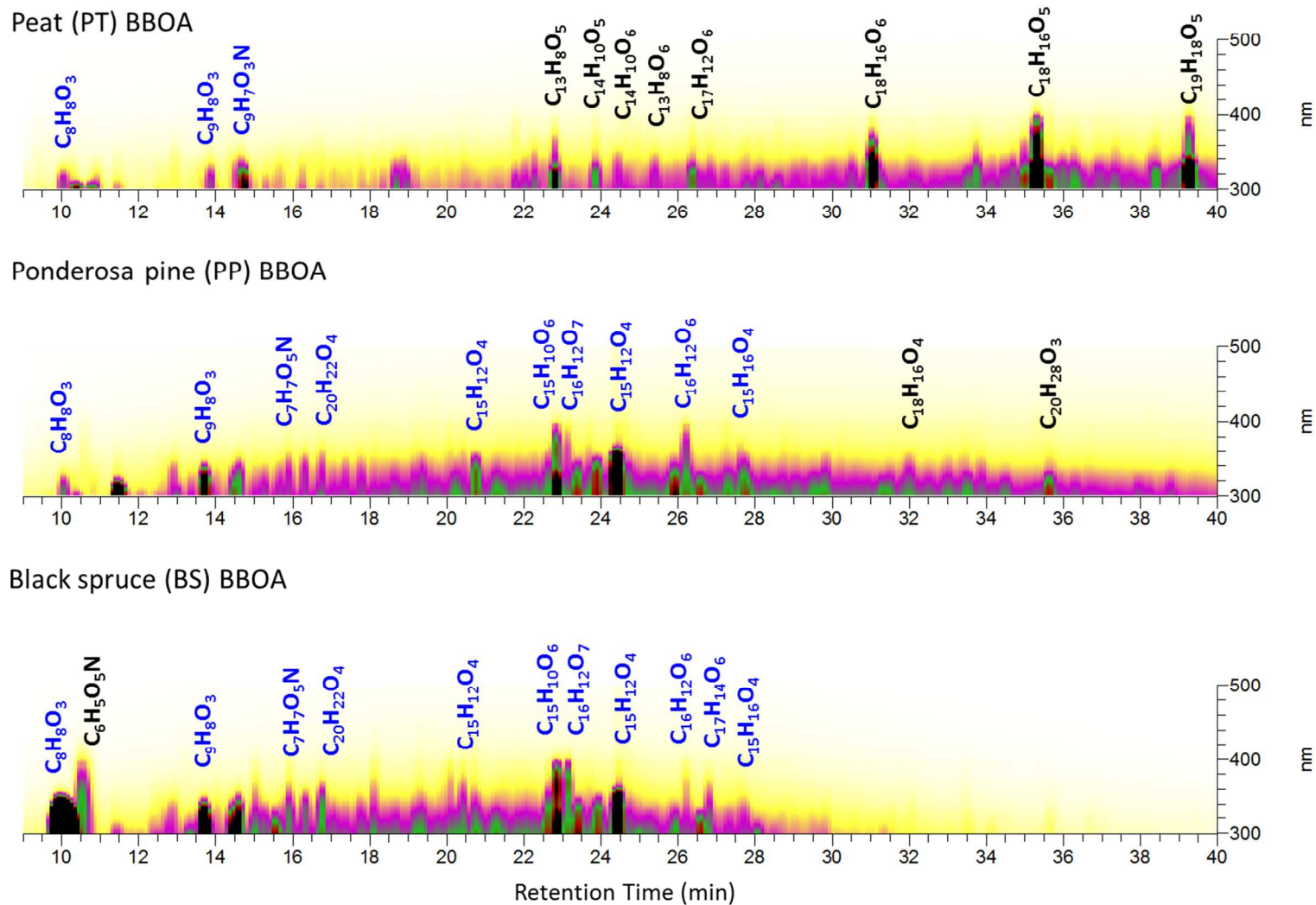


Figure S13. 10-40 min segments of HPLC/PDA chromatograms shown as density maps indicating strong BrC chromophores in the PT, PP, and BS BBOA samples. The elemental formulas of compounds corresponding to the major chromophores are listed accordingly. Blue color denotes chromophores common among different samples; black color indicates source specific chromophores.

Appendix I: Method for Testing the Stability of BrC Chromophores in Solution

The solutions of BBOA in 50 vol% water/acetonitrile solvent were irradiated in a standard 1 cm quartz cuvette from the side using radiation from a xenon arc lamp with a U-360 bandpass filter, a neutral-density filter (to reduce the power), and a lens (to make the cross section of the beam crossing the cell $\sim 1 \text{ cm}^2$). The cell was removed at regular time intervals, and the full absorption spectrum from 200-700 nm was taken with a Shimadzu 1800 spectrometer.

An azoxybenzene actinometer was used to measure the actinic flux ($\text{photons cm}^{-2} \text{ s}^{-1}$) of the lamp used for photolysis. This actinometer was chosen based on its quantum yield ($\phi=0.021$) being relatively independent of temperature and concentration. A 6.25 mM azoxybenzene solution with 12.5 mM potassium hydroxide, all in ethanol, was used as the actinometer, which was irradiated under the same conditions as BBOA samples. The concentration of the actinometer was chosen to result in similar absorbance levels to that of BBOA samples. The photoisomerization product of azoxybenzene absorbs at 458 nm with a molar extinction coefficient (ϵ) of $7600 \text{ L mol}^{-1} \text{ cm}^{-1}$, and can be used to estimate the actinic flux from the Xe lamp.

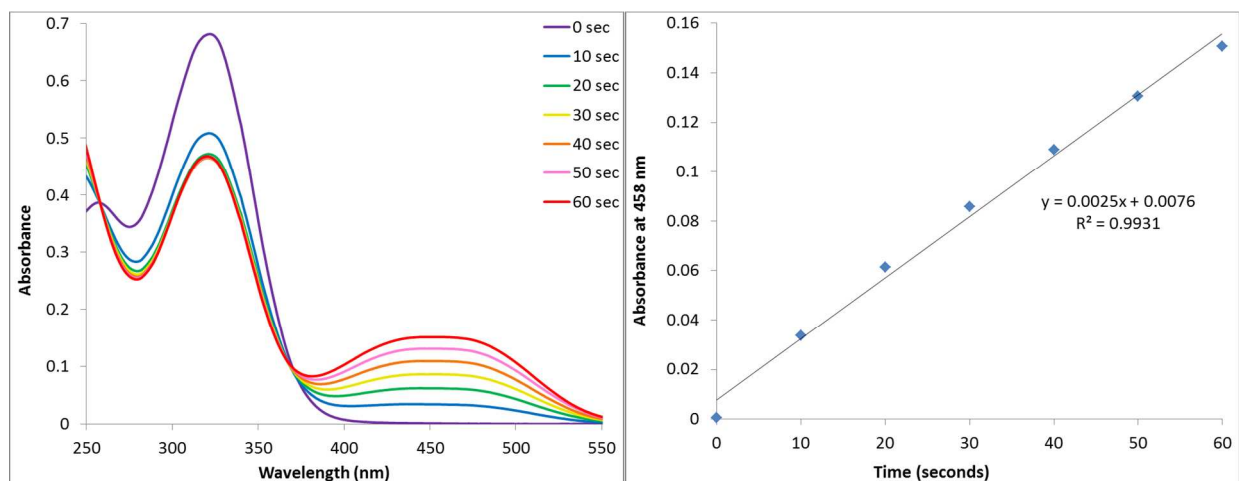


Figure S14. Spectra of actinometer at each photolysis point (left) and change in absorbance at 458 nm as a function of time (right) which was used to calculate the value for $\frac{dA_p}{dt}$.

Figure S14 shows typical spectra of the actinometer during photolysis. The time dependence of the 458 nm absorbance (A_p) can be used to determine rate of change in the concentration of the photoisomerization product (C_p) as a function of time using Beer's Law (Eqs. 1 and 2), where l is the path length of the cuvette and ϵ_p is the molar absorption coefficient of the product.

$$A_p = C_p \times \epsilon_p \times l \quad (\text{Eq. 1})$$

$$\frac{dC_p}{dt} = \frac{dA_p/dt}{\epsilon_p \times l} \quad (\text{Eq. 2})$$

The rate with which actinic photons passing through the cuvette are being absorbed by the solution, in moles of photons (= Einstein) per second, can be determined from the rate of the concentration change, the volume of solution being irradiated (V in liters) and the photoisomerization quantum yield (ϕ) (Eq. 3).

$$\text{Rate} \left(\frac{\text{photons}}{s} \right) = \frac{dC_p}{dt} \times \frac{V}{\phi} \quad (\text{Eq. 3})$$

This rate was then converted into the effective actinic flux of the lamp (F_{lamp}) using the area of the beam of light ($Area = 1 \text{ cm}^2$ based on the size of the beam) and Avogadro's number (N_A) (eq. 4).

$$F_{lamp} \left(\frac{\text{photons}}{\text{cm}^2 \times s} \right) = \frac{\text{Rate}}{\text{Area}} \times N_A \quad (\text{Eq. 4})$$

Note that equation 4 assumes that all actinic photons are absorbed by the solution, which is not the case. However, since the absorbance values of the actinometer solution and BBOA solution were similar, and we are only interested in the relative rates, we are not correcting for this effect.

The photolysis of Ponderosa Pine (PP) and Indonesian Peat (PT) was carried out using the same lamp conditions as the actinometer. The PP sample was irradiated for 1800 seconds and the PT was irradiated for 4500 seconds. The BBOA samples became somewhat less absorbing on average as a result of the UV exposure, as shown in Figure S15 for the PT sample. In addition, their Absorption Ångström Exponent (AAE) changed slightly (Figure S15 and Table S2). AAE was obtained by fitting logarithm of absorbance against logarithm of wavelength for the 300-500 nm wavelength range.

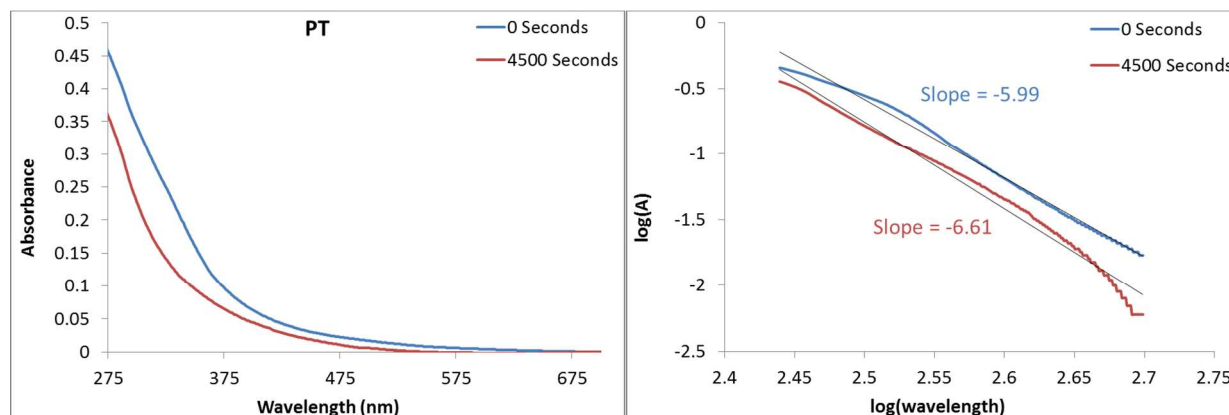


Figure S15. Left: Absorption spectra of the PT BBOA sample before and after UV irradiation. Right: the effect of the irradiation on the AAE of the PT BBOA.

Table S2. Half-lives ($t_{1/2}$) for the disappearance of the 300 nm absorbance measured in the experimental setup and estimated under the 24-hour averaged irradiation conditions in Los Angeles on June 30. AAE calculated were calculated for the 300-500 nm wavelength range.

Sample	Half-life measured under the lamp (hours)	Estimated half-life under the sun (hours)	AAE before irradiation	AAE after irradiation
PP	1.75	16.5	7.2	5.9
PT	1.70	16.0	6.0	6.6

The 300 nm absorbance of the BBOA samples was found to decrease with irradiation in most cases as shown in Figure S13, with photodegradation half-times of several hours.

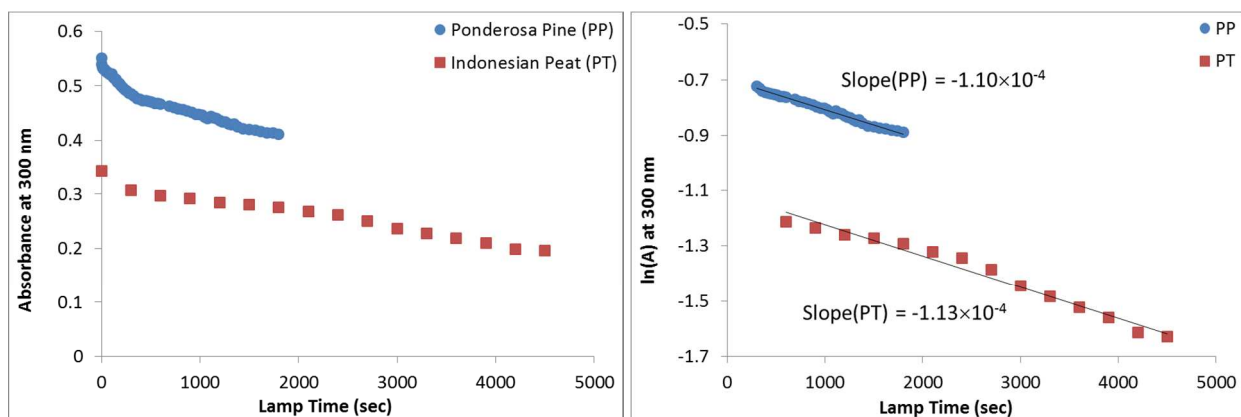


Figure S16. Left: Change in absorbance at 300 nm as a function of time exposed to the lamp for PP and PT BBOA samples. Right: Same on a natural log-linear scale, excluding the first 1000 s of data, where the absorbance changed the most rapidly. The slope of these curves can be converted into the half-live for the photodegradation assuming first order decay, $t_{1/2} = -\ln(2)/\text{slope}$.

To convert the photodegradation half-time into values representative of ambient UV irradiation, the average flux of the sun in a 24-hour period was calculated using the TUV model (http://cprm.acom.ucar.edu/Models/TUV/Interactive_TUV/). The model was used to obtain the solar spectrum at each hour on June 30 for Los Angeles, CA.

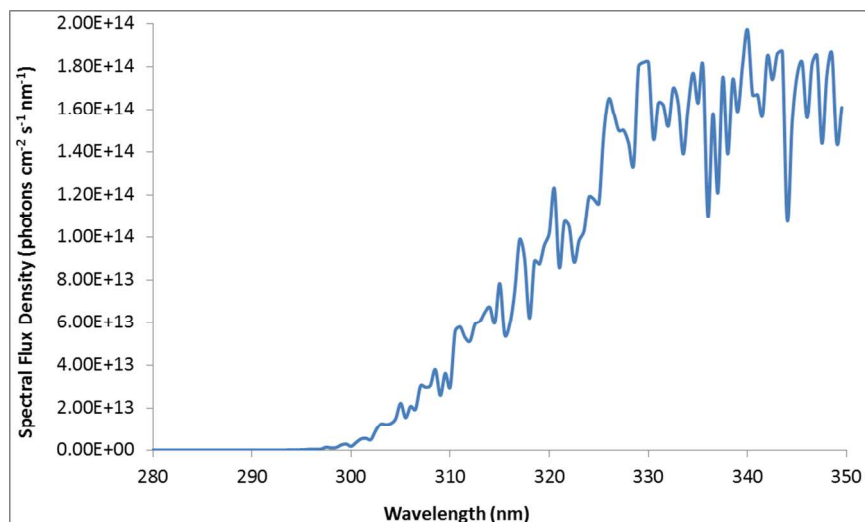


Figure S17. Solar spectral flux density in Los Angeles, CA on June 30 at 20 hours GMT (maximum flux).

These spectra were integrated from 280 to 350 nm using Mathematica in order to get the flux of the sun at each time point, which were then averaged to get an average solar flux (F_{sun}) (Eq. 5).

$$F_{sun} = \int_{280}^{350} F(\lambda) d\lambda \quad (\text{Eq. 5})$$

The upper limit in Eq. 5 is arbitrarily set to 350 nm because we assume that photons at longer wavelengths do not contribute substantially to the photodegradation.

Using the integrated actinic flux from the lamp ($F_{lamp} = 1.81 \times 10^{16}$ photon $\text{cm}^{-2} \text{s}^{-1}$) and the integrated actinic flux of the sun ($F_{sun} = 1.92 \times 10^{16}$ photon $\text{cm}^{-2} \text{s}^{-1}$), a factor for comparing the photolysis time of BBOA with the lamp to photolysis in the sun was determined to be 9.4 (Eq. 6 and 7). In other words, one hour under lamp is roughly equivalent to 9 hours under the sun.

$$Factor = \frac{F_{lamp}}{F_{sun}} \quad (\text{Eq. 6})$$

$$time_{sun} = Factor \times time_{lamp} \quad (\text{Eq. 7})$$

The PP's irradiation time of 1800 seconds is approximately equivalent to 4.7 hours under the sun using the conversion factor from Eq. 6. The PT's irradiation time of 4500 seconds is equivalent to about 11.8 hours in the sun using the same factor. In summary, the irradiation times used in this study would result in aging that BBOA would experience in about a day under daytime atmospheric conditions.

References

1. Stockwell, C. E.; Yokelson, R. J.; Kreidenweis, S. M.; Robinson, A. L.; DeMott, P. J.; Sullivan, R. C.; Reardon, J.; Ryan, K. C.; Griffith, D. W. T.; Stevens, L., Trace gas emissions from combustion of peat, crop residue, domestic biofuels, grasses, and other fuels: configuration and Fourier transform infrared (FTIR) component of the fourth Fire Lab at Missoula Experiment (FLAME-4). *Atmos Chem Phys* **2014**, *14*, (18), 9727-9754.
2. Stockwell, C. E.; Veres, P. R.; Williams, J.; Yokelson, R. J., Characterization of biomass burning emissions from cooking fires, peat, crop residue, and other fuels with high-resolution proton-transfer-reaction time-of-flight mass spectrometry. *Atmos Chem Phys* **2015**, *15*, (2), 845-865.
3. van der Werf, G. R.; Randerson, J. T.; Giglio, L.; Collatz, G. J.; Mu, M.; Kasibhatla, P. S.; Morton, D. C.; DeFries, R. S.; Jin, Y.; van Leeuwen, T. T., Global fire emissions and the contribution of deforestation, savanna, forest, agricultural, and peat fires (1997-2009). *Atmos Chem Phys* **2010**, *10*, (23), 11707-11735.
4. Bertschi, I.; Yokelson, R. J.; Ward, D. E.; Babbitt, R. E.; Susott, R. A.; Goode, J. G.; Hao, W. M., Trace gas and particle emissions from fires in large diameter and belowground biomass fuels. *J Geophys Res-Atmos* **2003**, *108*, (D13), 8472, DOI: 10.1029/2002JD002100.
5. Yokelson, R. J.; Burling, I. R.; Urbanski, S. P.; Atlas, E. L.; Adachi, K.; Buseck, P. R.; Wiedinmyer, C.; Akagi, S. K.; Toohey, D. W.; Wold, C. E., Trace gas and particle emissions from open biomass burning in Mexico. *Atmos Chem Phys* **2011**, *11*, (14), 6787-6808.
6. Lin, P.; Laskin, J.; Nizkorodov, S. A.; Laskin, A., Revealing Brown Carbon Chromophores Produced in Reactions of Methylglyoxal with Ammonium Sulfate. *Environ Sci Technol* **2015**, *49*, (24), 14257-14266.
7. Lin, P.; Liu, J. M.; Shilling, J. E.; Kathmann, S. M.; Laskin, J.; Laskin, A., Molecular characterization of brown carbon (BrC) chromophores in secondary organic aerosol generated from photo-oxidation of toluene. *Phys Chem Chem Phys* **2015**, *17*, (36), 23312-23325.
8. Pluskal, T.; Castillo, S.; Villar-Briones, A.; Oresic, M., MZmine 2: Modular framework for processing, visualizing, and analyzing mass spectrometry-based molecular profile data. *Bmc Bioinformatics* **2010**, *11*, 395-405.
9. Roach, P. J.; Laskin, J.; Laskin, A., Higher-Order Mass Defect Analysis for Mass Spectra of Complex Organic Mixtures. *Anal. Chem.* **2011**, *83*, (12), 4924-4929.
10. Koch, B. P.; Dittmar, T., From mass to structure: an aromaticity index for high-resolution mass data of natural organic matter. *Rapid Commun Mass Sp* **2006**, *20*, (5), 926-932.
11. Koch, B. P.; Dittmar, T., From mass to structure: an aromaticity index for high-resolution mass data of natural organic matter (vol 20, pg 926, 2006). *Rapid Commun Mass Sp* **2016**, *30*, (1), 250-250.
12. Li, Y.; Pöschl, U.; Shiraiwa, M., Molecular corridors and parameterizations of volatility in the chemical evolution of organic aerosols. *Atmos. Chem. Phys.* **2016**, *16*, (5), 3327-3344.
13. Shiraiwa, M.; Berkemeier, T.; Schilling-Fahnestock, K. A.; Seinfeld, J. H.; Pöschl, U., Molecular corridors and kinetic regimes in the multiphase chemical evolution of secondary organic aerosol. *Atmos Chem Phys* **2014**, *14*, (16), 8323-8341.